Synthesis, Characterization, and Metabolic Stability of Porphyrin−Peptide Conjugates Bearing Bifunctional Signaling Sequences

Martha Sibrian-Vazquez, Timothy J. Jensen, and M. Graça H. Vicente*

Department of Chemistry, Louisiana State University, Baton Rouge, Louisiana 70803

Received August 23, 2007

A series of four porphyrin−peptide conjugates bearing one linear bifunctional sequence containing a cell penetrating peptide (CPP) and a nuclear localization signal (NLS) were synthesized and their in vitro biological and stability properties investigated. All conjugates accumulated within human HEp2 cells to a significantly higher extent than their porphyrin−PEG precursor, and the extent of their uptake and cytotoxicity depends on the nature and sequence of the amino acids. Conjugates **2** and **5** bearing a NLS-CPP accumulated the most within cells and were the most phototoxic ($IC_{50} \approx 7$ μM at 1 J/cm^2). All conjugates localized preferentially within the cell lysosomes, and in addition, conjugate **2** was also found in the ER. All conjugates were highly stable under nonenzymatic conditions, but their peptide sequences were cleaved to some extent (ca. 50% after 24 h) by proteolytic enzymes, such as cathepsin B, cathepsin D, prolidase, and plasmin.

Introduction

Photodynamic therapy (PDT)[a,1,2] and boron neutron capture therapy (BNCT)[3] are binary therapies for cancer treatment that involve the activation of a tumor-localized sensitizer with red light (in PDT) or with low energy neutrons (in BNCT). The cytotoxic agents generated in PDT are reactive oxygen species (ROS), mainly $^1O_2$, whereas in BNCT the high linear energy transfer particles $^4He^{2+}$ and $^7Li^{3+}$ are formed via the ^{10}B-neutron capture nuclear reaction. These cytotoxic species have limited ranges in tissue (approximately 0.1 μm for $^1O_2$, 9 μm for $^4He^{2+}$, and 5 μm for $^7Li^{3+}$), and therefore, the toxic effect is restricted to their site(s) of generation. As a consequence, the biological efficacy of porphyrin-based sensitizers depends on both their selectivity for tumor tissue and their subcellular distribution.[4,5] In order to increase the tumor specificity and water solubility of sensitizers several methodologies have been explored, including the use of lipid vehicles such as Cremophor EL and liposomes[6] and the conjugation to biological molecules, such as proteins, antibodies, and carbohydrates.[7–14] A particularly attractive strategy for increasing cellular uptake and delivery of therapeutic drugs into specific organelles is the use of peptide signaling sequences, such as a cell penetrating or fusogenic peptide (CPP), a nuclear localization signal (NLS), and bifunctional signaling sequences containing, for example, both a CPP and a NLS. CPPs are minimum sequences required for rapid and efficient cellular internalization normally found in the transduction domain of proteins;[15] examples of CPP include the *Drosophila* homeotic transcription protein antennapedia (penetratin, Antp),[16] the human immunodeficiency virus I transcriptional activator (HIV-1 Tat),[17] the herpes-virus derived VP22,[18] and synthetic arginine-rich polypeptides.[19] NLS characteristically contain short sequences of positively charged amino acids (arginine and/or lysine) and are divided into monopartite and bipartite depending on whether they contain one or two clusters of at least four cationic amino acids.[20] Among the NLS, the best characterized monopartite is the sequence PKKKRKV derived from the simian virus 40 (SV40) large T antigen,[20] and the best characterized bipartite is the nucleoplasmin with the minimal sequence KRPAATKKAGQAKKKL.[22] Porphyrin conjugates bearing the NLS SV40 have been reported, and in all cases, the conjugates showed increased photosensitizing activity as a consequence of nuclear delivery, when compared with the corresponding unconjugated porphyrins.[21,23–25] We have previously investigated a series of porphyrin conjugates bearing either the NLS SV40 or the CPP HIV-1 Tat 48–60 sequences.[21] Although these conjugates were not found in the nuclei of HEp2 cells, the porphyrin−CPP exhibited enhanced cellular uptake and the porphyrin−NLS enhanced phototoxicity, compared with the unconjugated porphyrin. These studies showed that the biological efficacy of porphyrin-peptide conjugates depends on the nature and sequence of the amino acids on the peptide chain, the nature of the substituents at the periphery of the porphyrin macrocycle and the overall charge and amphiphilicity of the conjugate. In our continuing design and investigation of photosensitizers with enhanced biological efficacy, we hypothesized that a cell-targeted porphyrin-peptide conjugate bearing a linear bifunctional CPP−NLS or NLS−CPP peptide, with minimum sequences for cell membrane translocation and for directing the movement of the molecule into the cell nucleus, could show both increased cellular uptake and phototoxicity. Herein, we report the synthesis, characterization, cellular studies and metabolic stability of a series of four new porphyrin−peptide conjugates containing bifunctional peptide sequences composed of an amphiphatic and cationic CPP and a NLS corresponding to either the SV40 large T antigen or the nucleoplasmin sequences. A similar approach has been used for the preparation of conjugates of chlorin-e_6 to multiple pentalysine-SV40 peptides;[25] these conjugates showed enhanced biological efficacy

* To whom correspondence should be addressed. Phone: 225-578-7405. Fax: 225-578-3458. E-mail: vicente@lsu.edu.

[a] Abbreviations: CPP, cell penetrating peptide; NLS, nuclear localizing signal; HOBt, 1-hydroxybenzotriazole; ROS, reactive oxygen species; CCA, α-cyano-4-hydroxycinnamic acid; TFA, trifluoroacetic acid; DIEA, *N,N*-diisopropylethylamine; TBTU, 2-(1*H*-benzotriazole-1-yl)-1,1,3,3-tetramethyluronium tetrafluoroborate; Boc, *tert*-butoxycarbonyl; HEPES, 4-(2-hydroxyethyl)-1-piperazineethanesulfonic acid; PBS, phosphate-buffered saline; FBS, fetal bovine serum; DMEM: Dulbecco's Modified Eagle's Medium; MEM, minimal essential medium; PEG, poly(ethylene glycol); TIS, triisopropylsilane; Fmoc, 9-fluorenylmethoxycarbonyl; TFE, trifluoroethanol; SDS, sodium dodecylsulfonate; PAL-PEG-PS, peptide amide linker-poly(ethylene glycol)-polystyrene; PyBOP, benzotriazol-1-yloxytripyrrolidinophosphonium hexafluorophosphate.

10.1021/jm701050j CCC: $40.75
Published on Web 04/22/2008

compared with chlorin-e_6 but were difficult to synthesize, purify, and characterize as a result of their high molecular weights.

Results and Discussion

1. Synthesis and Characterization. The specific delivery of porphyrin-based sensitizers into cancer cells is determined by their ability to cross the plasma membrane, which in turn depends on the macrocycle structural and physicochemical properties. We hypothesized that a porphyrin−peptide conjugate bearing a bifunctional CPP−NLS or NLS−CPP signaling sequence may show increased tumor cell uptake and enhanced photodynamic activity. We anticipated that the CPP sequence would direct the conjugate's movement across the cellular membrane into the cytoplasm, by either transient membrane permeabilization or receptor-mediated endocytosis, and the NLS would favor the conjugate's preferential localization within the cell nuclei and other sensitive organelles. We therefore designed and synthesized four porphyrin−bifunctional peptide conjugates (**2**−**5**) bearing both CPP and NLS sequences. Bifunctional peptides are generally classified as hydrophobic, amphiphatic, and cationic, depending on the nature of the amino acid sequence.[24–29] In order to balance the hydrophobic nature of the porphyrin macrocycle we selected the amphiphatic CPP sequences corresponding to either penetratin, the fusion peptide of HIV-1 gp41, or the HIV-1 Tat 48–60. Primary amphiphatic peptides result from the sequential assembly of hydrophobic and hydrophilic domains; the first domain is required for membrane anchoring and complex formation with hydrophobic molecules while the second domain enhances water solubility, induces complex formation with hydrophilic, negatively charged molecules, and directs the molecule to a subcellular compartment. There are three major families of primary amphiphatic peptides containing a common hydrophilic domain corresponding to the NLS SV40. These peptides bear a WSQ sequence which acts as a linker between the hydrophilic and hydrophobic domains, thereby maintaining their integrity.[26] Such peptides covalently linked through the cysteine residue, have been used for the intracellular delivery of oligonucleotides and porphyrin derivatives.[24] The resulting conjugates were found to be toxic in the dark at concentrations higher than 10 μM, probably as a consequence of pore formation and subsequent membrane depolarization. Penetratin is an amphiphilic peptide derived from the third helix of the DNA binding domain of *Drosophila* antennapedia [Antp(43–58), penetratin]. It contains cationic amino acids that interact with DNA and hydrophobic amino acids that interact with other helices to maintain the DNA–protein complex structure. The translocation activity of penetratin depends on the distribution of the positively charged residues and of the two tryptophan amino acids that reside on the theoretical helical structure.[16] The cationic peptide sequence HIV-1 Tat 48–60 has been extensively used for the efficient delivery of drugs into cells.[17,19] It can play a double targeting role by initially delivering its cargo into the cytosol and then into the nucleus. We have previously observed that a porphyrin-HIV-1 Tat 48–60 conjugate shows enhanced cellular uptake than the unconjugated porphyrin and that the cell nucleus is not its main site of subcellular localization.[21] In the present study, we hypothesized that the coupling of a photosensitizer to both CPP and NLS signaling sequences might result in an enhancement of its biological efficacy. In eukaryotic cells, most of the natural NLS are bipartite consisting of two short cationic domains separated by a spacer of 10−12 residues. The best characterized bipartite NLS is that of nucleoplasmin with the minimal sequence KRPAATKKAGQAKKKL; among the monopartite

Scheme 1. Synthetic Route to Porphyrin−Peptide Conjugates **2**–**5**

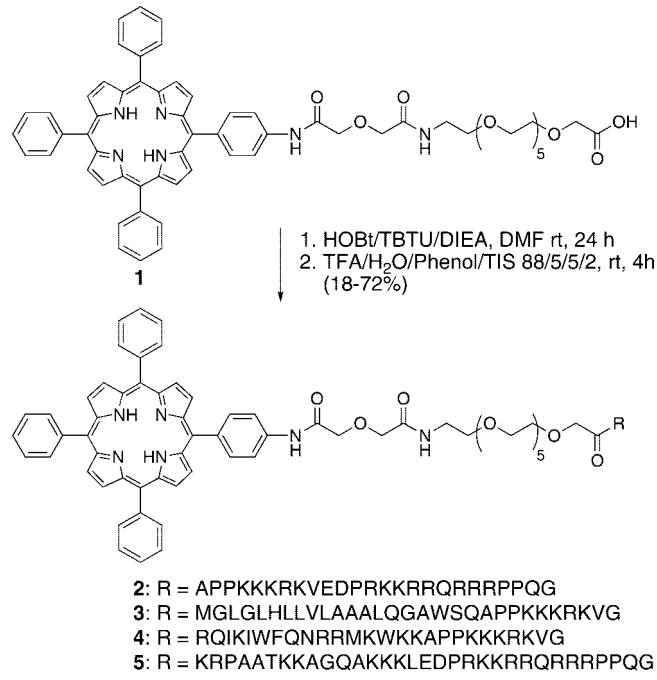

NLS, the best characterized is the short sequence PKKKRKV derived from the SV40 large T antigen.[20] We therefore chose to couple the NLS sequences corresponding to the SV40 large T antigen and the bipartite nucleoplasmin to the above CPP sequences in order to produce a single chain peptide vector (CPP−NLS or NLS−CPP). The resulting peptide vectors correspond to the amphiphatic sequences MGLGLHLLVLAAALQGAWSQAPPKKKRKVG, a modified version of that previously reported[24] which contains a longer sequence for the hydrophilic SV40 large T antigen, RQIKIWFQNRRMKWKKAPPKKKRKVG (penetratin-SV40), and the cationic peptides KRPAATKKAGQAKKKLEDPRKKRRQRRRPPQG (nucleoplasmin-HIV-1 Tat 48–60) and APPKKKRKVEDPRKKRRQRRRPPQG (SV40−HIV-1 Tat 48–60). The side-protected peptide sequences were synthesized using Fmoc-solid phase methodology, as we have previously reported.[21] After the coupling of the last residue, the Fmoc-group was removed and the free amino group was used in the conjugation reaction to porphyrin **1**,[21] a carboxylate-terminated pegylated porphyrin. The PEG chain in porphyrin **1** was designed to act as a spacer between the porphyrin and the peptide sequence, in order to reduce intra- and intermolecular interactions and to improve water solubility.[30–32] Conjugates **2**–**5** were synthesized as shown in Scheme 1 using our previous reported coupling methodology.[21,30] In brief, PEG-porphyrin **1** was activated as the hydroxybenzotriazole (HOBt) ester and coupled to the free amino group of the protected peptidyl PAL-PEG-PS resin using TBTU. After cleavage and deprotection from the solid support using TFA/Phenol/H_2O/TIS 88/5/5/2, the water-soluble porphyrin-peptide conjugates **2**−**5** were isolated by reversed-phase HPLC in yields ranging from 18 to 72%. Based on the reversed-phase HPLC retention times, the hydrophobic character of the porphyrin-peptide conjugates follows the order **3** > **4** > **2** > **5**.

2. CD Studies. Conformational studies of the peptides conjugated to porphyrin **1** were conducted in different media, including aqueous and membrane mimicking environments (see Figure 1 and Table 1). In aqueous solution at pH 5.00, all porphyrin−peptide conjugates show negative Cotton effects at 198–207 nm, which are characteristic of a random coil

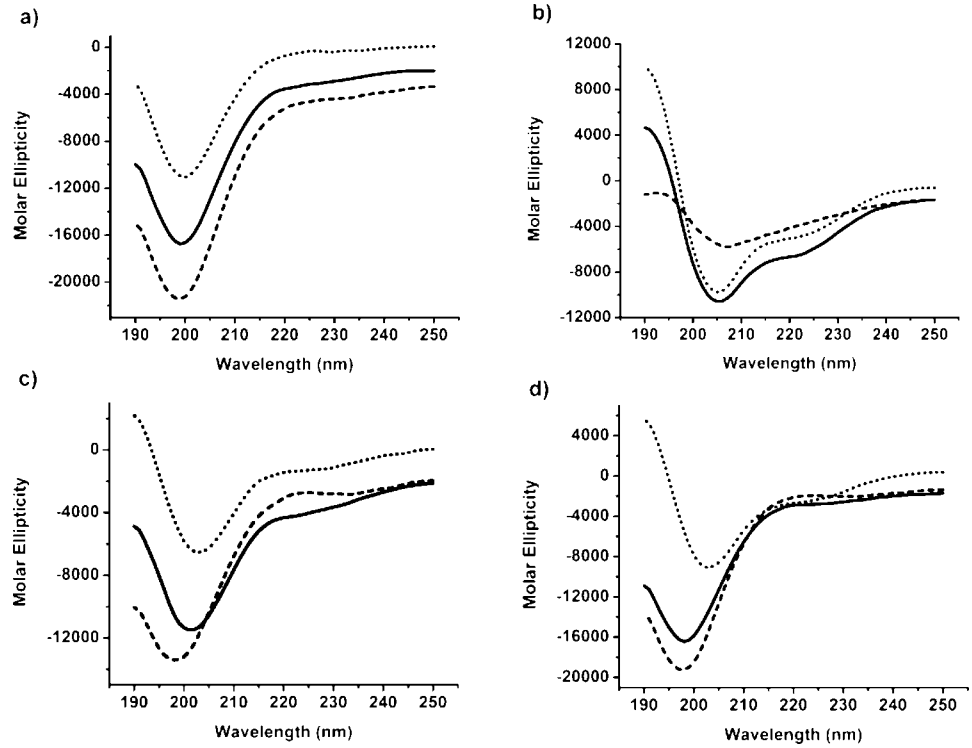

Figure 1. CD spectra in the amide region of (a) **2**, (b) **3**, (c) **4**, and (d) **5**. TFE/H_2O, pH 7.00 (full line), 50 mM NaH_2PO_4, pH 5.00 (dash line), 100 mM SDS/H_2O (dot line). Conjugate concentration 20 μM. The ellipticity is given in deg cm^2 dmol^{-1}, cell path 1 mm, temperature 25 °C.

Table 1. Molar Ellipticity of Porphyrin−Peptide Conjugates **2**–**5**

	molar ellipticity (deg cm^2 dmol^{-1})		
ID	50 mM NaH_2PO_4, pH 5.00	H_2O/TFE 9/1, pH 7.00	100 mM SDS/ H_2O, pH 3.7
2	−16740 (199 nm)	−21440 (199 nm)	−11070 (200 nm)
3	−5780 (207 nm)	−10600 (205 nm)	−9760 (205 nm)
		−6610 (221 nm)	−5000 (221 nm)
4	−13410 (198 nm)	−11490 (201 nm)	−6540 (203 nm)
			−1360 (222 nm)
5	−19230 (198 nm)	−16430 (198 nm)	−9110 (203 nm)
			−2600 (222 nm)

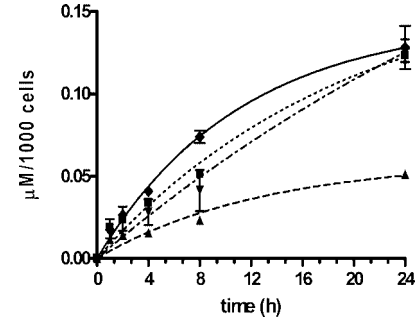

Figure 2. Time-dependent uptake of porphyrin conjugates **2** (dotted line), **3** (dash line), **4** (dot-dash line), and **5** (full line) at 10 μM by HEp2 cells.

conformation. For example, for polylysine at pH 7, $[\theta] = -41900$ deg cm^2 dmol^{-1} at 197 nm.[33] In membrane mimicking environments, in the presence of TFE or SDS, an α-helix structure characterized by two negative bands at 205 and 221 nm, associated with a positive band at 193 nm, is induced for conjugate **3**. For example, for polylysine at pH 7, $[\theta] = 76900$ deg cm^2 dmol^{-1} at 191 nm, $[\theta] = -32600$ deg cm^2 dmol^{-1} at 208 nm, and $[\theta] = -35700$ deg cm^2 dmol^{-1} at 222 nm.[33] In the presence of TFE, conjugates **4** and **5** adopt a random coil conformation as observed by the negative band at 201 and 198 nm, respectively; however, in the presence of SDS, an α-helix conformation is induced for both conjugates as observed by the presence of two negative bands at 203 and 222 and a positive band at 193 nm. These results show, with the exception of conjugate **2**, that conjugates **3**−**5** adopt different conformations depending on the nature of their environment. These differences may be attributed to the hydrophobic/hydrophilic character of the amino acid sequence in each peptide. While the peptide sequence in conjugate **2**, contains mainly cationic residues (K and R), the peptide sequences in conjugates **3**−**5** contain a larger number of hydrophobic amino acids, which may be responsible for the α-helix conformation induced in the membrane mimicking environments. We also observed that the coupling of an NLS to a CPP does not significantly influence the preferred conformation of each individual sequence. Our results are in agreement with previous studies showing that in the crystal structures of the kariopherin α-SV40 and the importin α-nucleoplasmin (155–170, KRPAATKKAGQAKKKK) complexes, the peptide sequences adopt extended conformations.[34,35] On the other hand, CD investigations of the Tat protein have shown that the highly basic region from 48 to 60 (PRKKRRQRRRPPQ) adopts an extended conformation due to the electrostatic repulsion between the positively charged side groups.[36] In contrast, CD and NMR studies have shown that the penetratin sequence [Antp(43–58)] usually adopts an α-helix or β-sheet conformation when associated with vesicles,[37] and that the amphiphatic peptide sequence on conjugate **3** adopts a random coil conformation in water and an α-helix in membrane mimicking environments.[38]

3. Cell Culture Studies. 3.1. Time-Dependent Cellular Uptake. The time-dependent uptake of conjugates **2**−**5** by human HEp2 cells was investigated at a concentration of 10 μM, and the results obtained are shown in Figure 2. We have recently reported the cellular properties of the PEG-porphyrin **1** using the same cell line;[39] the biological properties of the

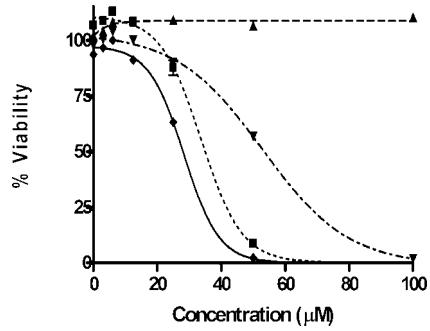

Figure 3. Dark toxicity of porphyrin conjugates **2** (dotted line), **3** (dash line), **4** (dot-dash line), and **5** (full line) toward HEp2 cells using the Cell Titer Blue assay.

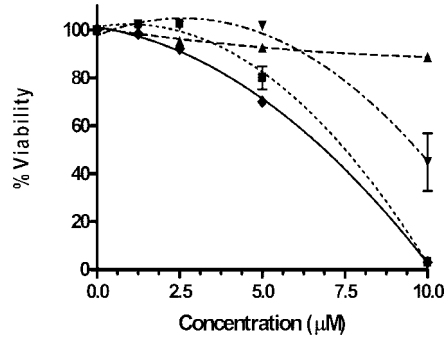

Figure 4. Phototoxicity of porphyrin conjugates **2** (dot line, squares), **3** (dash line, triangles), **4** (dot-dash line, inverted triangles), and **5** (full line, diamonds) toward HEp2 cells using 1 J/cm^2 dose light.

PEG-free porphyrin precursor were not investigated due to its poor solubility in water. The cellular uptake of conjugates **2**−**5** was 3−8 times higher than that of porphyrin **1** at all time points studied and depends on the nature and sequence of the amino acid residues in the peptide chain and on the overall hydrophobic character of the conjugate. Interestingly, the uptake of the conjugates decreased with increasing hydrophobic character (as determined based on HPLC retention times); the most hydrophobic conjugate **3** accumulated the least within cells at all time points studied, whereas the least hydrophobic conjugate **5** accumulated the most. After 24 h, the amount of conjugates **2**, **4**, and **5** found within cells was similar and about 3 times higher than that of conjugate **3**. It is worth noting that the conjugates containing the HIV-1 Tat 48–60 (rather than the HIV-1 gp41 or penetratin) and NLS-CPP rather than CPP-NLS sequences (i.e., **5** and **2**) accumulated the most within HEp2 cells. Our results are in agreement with previous studies showing that the nature and sequence of the cationic amino acid residues in the peptide chain is crucial for efficient translocation across cellular membranes. Cationic peptides bearing multiple arginine residues tend to accumulate to a greater extent than peptides based on lysine residues. It has been postulated that positively charged guanidinium groups from the arginine residues play an important role in facilitating cellular uptake, probably by forming bidentate hydrogen bonds with membrane-containing phosphate groups.[19]

3.2. Cytotoxicity. The dark cytotoxicity and phototoxicity of the new porphyrin conjugates were evaluated in human HEp2 cells exposed to increasing concentrations of each conjugate for 24 h, as shown in Figures 3 and 4, respectively. Conjugate **3** accumulated the least within cells and shows no toxicity at concentrations up to 100 μM in the dark and no phototoxicity upon exposure to low light dose (1 J/cm^2) up to 10 μM concentrations. On the other hand, conjugates **2**, **4**, and **5** were found to be moderately toxic in the dark, with IC_{50} values of 34, 53, and 27 μM, respectively. Upon exposure to a low light dose (1 J/cm^2), conjugates **2**, **4**, and **5** showed IC_{50} values of 7.5, 9.3, and 6.9 μM, respectively. The phototoxicity order followed that of cellular uptake, i.e. **5** > **2** > **4** > **3**. Conjugates **5** and **2** bearing a NLS (nucleoplasmin or SV40, respectively) followed by the HIV-1 Tat 48–60 peptide sequences accumulated the most within cells and were the most phototoxic. Of the two porphyrin−CPP−NLS (SV40) conjugates **3** and **4**, that containing penetratin (i.e., **4**) was significantly more cytotoxic than that bearing the CPP derived from HIV-1 gp41 (i.e., **3**). Our results show, as previously observed,[4] that the amount of sensitizer accumulated within cells, as well and its subcellular distribution (vide infra) determine its phototoxicity and therefore its biological efficacy.

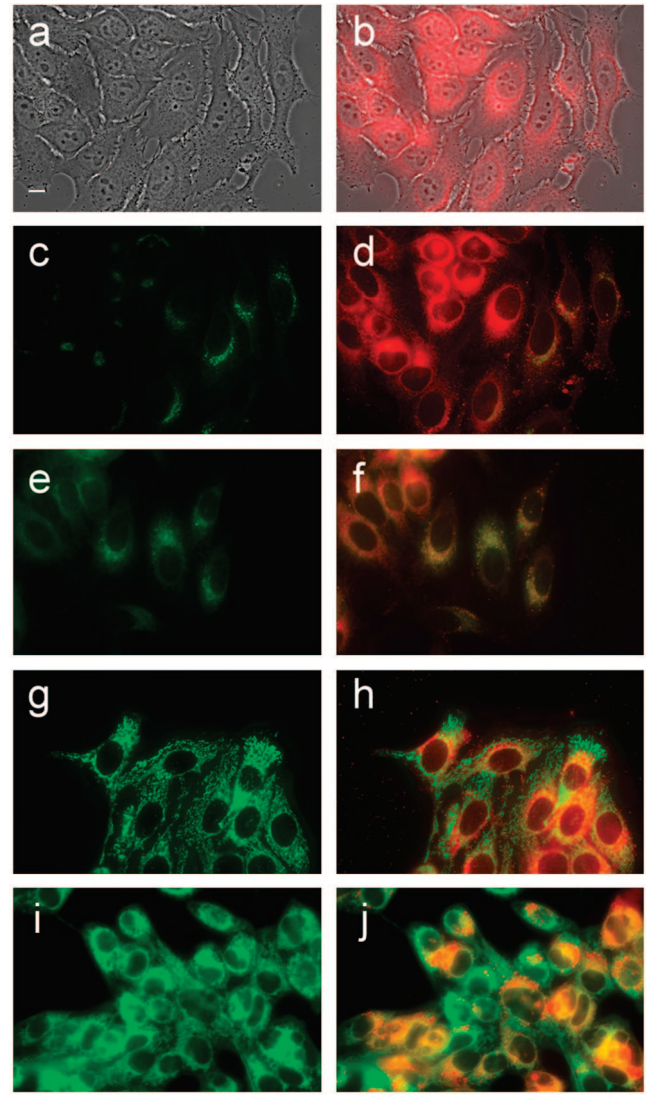

Figure 5. Subcellular localization of conjugate **2** in HEp2 cells at 10 μM for 18 h: (a) phase contrast, (b) overlay of **2** fluorescence and phase contrast, (c) BODIPY Ceramide, fluorescence, (e) LysoSensor Green fluorescence, (g) MitoTracker Green fluorescence, (i) $DiOC_6$ (d), (f), (h), and (j) overlays of organelle tracers with **2** fluorescence. Scale bar: 10 μm.

3.3. Intracellular Localization. The preferential sites of subcellular localization of conjugates **2**−**5** in HEp2 cells at a concentration of 10 μM were investigated using fluorescence microscopy. Figure 5 shows the fluorescence pattern observed for conjugate **2** and its overlay with the organelle specific fluorescent probes LysoSensor Green (lysosomes), Mitotracker

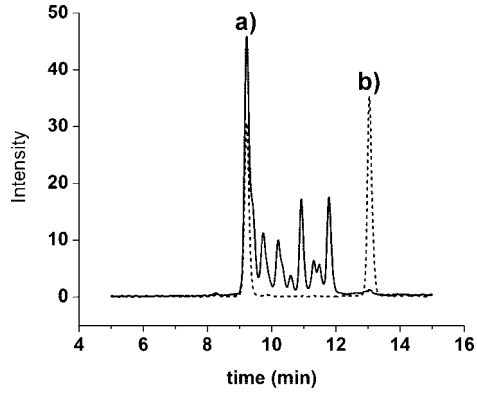

Figure 6. HPLC trace of HEp2 cellular extract of conjugate **5** after 24 h (full line) and HPLC trace for a control mixture of conjugate **5** (a), t_r = 9.21 min and porphyrin **1** (b), t_r = 13.04 min (dotted line).

Green (mitochondria), $DiOC_6$ (ER), and BODIPY FL C_5-ceramide (Golgi complex). Similar images were obtained for conjugates **3**−**5** (see the Supporting Information, Figures S1−S3). We observed that conjugates **3** and **4** collected in large vesicles, and in addition, some conjugate **4** was also found in the lysosomes. The preferential sites of intracellular localization of conjugate **5** are the cell lysosomes. Conjugate **2** was mainly found in the lysosomes and the ER. These results suggest that the sites of subcellular localization of porphyrin−peptide conjugates are determined by their overall charge and cellular uptake mechanism. Although conjugates **2**−**5** all contain a NLS sequence, either the SV40 or the nucleoplasmin sequences, the cell nucleus is not their main localization site; it is possible, however, that in the case of **2** and **5** bearing the highly cationic HIV-1 Tat sequence, a small amount of conjugate localizes near or within the nucleus, thus explaining their higher phototoxicity in comparison with **3** and **4**. It has been reported that the conjugate of the cationic porphyrin tris-MePy-TPP-I to the amphiphatic peptide MGLGLHLLVLAAALQGAWSQAKK-KRKVC via a cysteamide bond is delivered into the nuclei of fibroblasts HS68 and lymphocytic leukemia L1210 cells.[24] Therefore, we also investigated the subcellular distribution of conjugates **2**–**5** in fibroblasts cell line V79, but results similar to those described above including no nuclear localization were observed (results not shown). Our results and previous studies[21,30] indicate that the intracellular localization of porphyrin−peptide conjugates depends on the nature and sequence of amino acids on the peptide sequence and the overall charge of the conjugate; thus, conjugates bearing short sequences containing one to four cationic amino acids tend to localize preferentially in the lysosomes,[30] whereas those bearing arginine-rich peptides such as the HIV-1 Tat 48–60 or octaarginine localize preferentially in the ER.[21] Both the lysosomes and ER are important targets for the PDT-induced initiation of apoptosis.[40,41]

4. Metabolic Stability. The biological efficacy of porphyrin sensitizers depends on their specific delivery into tumor cells and into sensitive organelles.[4] We have previously observed[21] that porphyrin−peptide conjugates containing a CPP sequence show enhanced cellular uptake whereas those containing a NLS (e.g., SV40) show enhanced phototoxicity. However the biological efficacy of peptide conjugates depends on their stability under physiological conditions, i.e., their ability to maintain their chemical integrity until the targeted tumor cells and organelles are reached.[42] Therefore we investigated the stability of porphyrin-peptide conjugates **2**-**5** under both enzymatic and nonenzymatic conditions, using MALDI-TOF mass spectrometry and HPLC. The results obtained are shown in Figure 6 and in the Supporting Information, Figures S4−S7 and Tables S1 and S2.

The chemical (nonenzymatic) hydrolysis of porphyrin−peptide conjugates was investigated at the pH values 7.4 and 5.0, since there is a decrease in pH as the molecules cross the plasma membrane of tumor cells into the endosomes and lysosomes (pH 6.5–4.0). Nonenzymatic peptide hydrolysis is a slow process that can be catalyzed by acids, bases, and metal complexes; depending on the conditions, hydrolysis of peptide substrates with a half-time of approximately 2 days up to 7 years have been reported.[43,44] Upon incubation of conjugates **2**−**5** for 24 h at 37 °C, at pH 7.4 and 5.0, we observed no degradation by MALDI-TOF mass spectra, as shown in Figure S4 of the Supporting Information for conjugate **5**. At both pH values a major peak at *m*/*z* 4812 corresponding to protonated conjugate **5** ($M + H^+$) was observed, along with a minor peak at *m*/*z* 2407 at pH 5.0 due to the ($M + 2H^+$) ion. These results clearly indicate that the porphyrin-peptide conjugates are chemically stable under the conditions tested, since no degradation or hydrolysis products were observed by mass spectrometry.

The enzymatic stability of the porphyrin−peptide conjugates **2**−**5** was evaluated using enzymes cathepsin B, cathepsin D, prolidase, and plasmin, all known to be overexpressed in cancer cells.[45–48] While cathepsin enzymes are active at pH 5–6, prolidase and plasmin are active at pH 7–8. The lysosomal endoproteinase cathepsin D normally shows specificity toward bonds between hydrophobic amino acids, and although it is relatively inactive toward low molecular weight substrates, certain short peptides containing five or more residues, e.g., GFLGF, are cleaved by this enzyme. Cathepsin B is involved in the intracellular digestion of extracellular proteins taken up by endocytosis, and many proteins are known to be degraded by this enzyme. The optimum pH for cleavage of low molecular weight peptide substrates by this enzyme is about 6.0.[45] Prolidase is a widely occurring mammalian dipeptidase that normally splits aminoacylprolines into the constituent amino acids. Apparently, this enzyme is unique because many other catabolic enzymes are unable to cleave the RCO-proline tertiary carboxamide linkage. Small noncharged amino acids such as glycine or leucine are preferred by this enzyme.[46,47] Plasmin is a serine protease that is a primary constituent of the proteolytic cascade. It plays a vital role in the breakdown of the basement membrane and facilitates angiogenesis and the migration of cancer cells. The proteolytically active form of plasmin is localized at the tumor level since it is formed from its inactive proenzyme form plasminogen by urokinase-type plasminogen activator, produced by cancer and/or stroma cells. Peptide sequences DAFK and DVLK have been identified as substrates for this enzyme.[48] The porphyrin−peptide conjugates **2**−**5** were incubated at 37 °C for 24 h with each of these enzymes in their activated form and corresponding optimum pH. At the end of this period, the enzymatic activity was quenched and the reaction mixtures were analyzed by HPLC and MALDI-TOF mass spectrometry.[49] In all cases, the peptide sequences of conjugates **2**−**5** were hydrolyzed to some extent (see Figure S5 of the Supporting Information). Several reaction products containing the porphyrin macrocycle were identified (see Tables S1 and S2 with possible hydrolysis products in the Supporting Information). Cathepsin B hydrolyzed the peptide group of conjugates **2**−**5** to a higher extent than cathepsin D, plasmin, and prolidase. The hydrolysis of the peptide groups was dependent on their sequences, and no specific pattern was observed, possibly as a result of the large active site in these enzymes. It has been determined that the reactivity of a certain bond in a protein or

peptide depends not only on the two residues forming the bond but also on the residues in its neighborhood that occupy adjacent subsites. Our results indicate that the integrity of the peptide chains in the porphyrin−peptide conjugates may be compromised in the presence of proteolytic enzymes, since the conjugates are suitable substrates for these enzymes.

To further corroborate the metabolic stability of conjugates **2**−**5** toward enzymatic hydrolysis, and since the kind and concentration of proteolytic enzymes is determined by the type of cancer cell, we conducted time-dependent experiments using human HEp2 cells, mass spectrometry and HPLC. Figure S6 of the Supporting Information shows the results obtained with conjugate **5** upon examination of the cellular extracts using MALDI-TOF mass spectrometry. At all times investigated (up to 24 h), a peak corresponding to intact conjugate was seen by mass spectrometry. In addition, after 1 h, the mass spectrum of the cellular extract of HEp2 cells treated with conjugate **5** displays minor peaks at *m*/*z* 1359 and 4189. After 2 h, a main peak at *m*/*z* 1518 and minor peaks at *m*/*z* 1066, 1194, and 1692 were observed, corresponding to porphyrin−PEG−KRPA, porphyrin−PEG, porphyrin−PEG−K, and porphyrin−PEG−KRPAAT, respectively. The same pattern was observed after 4, 8, and 24 h; however, the intensity of the peaks at *m*/*z* 1066, 1194, and 1692 slightly increased over time. None of these peaks were present in the mass spectrum of an extract obtained from a solution of the conjugate in cell culture medium containing no cells. The reversed-phase HPLC of the cellular extract after 24 h shows the presence of conjugate **5** (t_R = 9.21 min, ca. 50%) and degradation products, including PEG−porphyrin **1** (t_R = 13.04 min), as shown in Figure 6. All the degradation products present in the 24 h cellular extract contain the porphyrin macrocycle since the UV–vis spectra of each individual peak exhibited the characteristic Soret band with a maximum at 421–431 nm (see Figure S7 of the Supporting Information). Our results indicate that the peptide chains of porphyrin−peptide conjugates are subject to some metabolic degradation within HEp2 cells under the conditions investigated, by proteolytic enzymes present in this cell line. As a consequence, we anticipate that the biological efficacy of porphyrin−peptide conjugates containing organelle-specific sequences will depend on the nature and extent of the enzymatic hydrolysis of their signaling sequences within tumor cells. These results are in agreement with the intracellular localization patterns observed for conjugates **2**–**5** (vide supra) since no nuclear localization was observed for any of the NLS-containing conjugates. It is possible that porphyrin−peptide conjugates **2**−**5** are internalized via an endocytotic mechanism prior to their cleavage, which is consistent with their enhanced cellular uptake compared with unconjugated porphyrin−PEG **1**, and their preferential localization within endosomes and lysosomes. Once inside the cells, it is possible that the conjugates remain trapped in the endosomes and lysosomes and their peptide sequences are degraded to some extent by proteolytic enzymes present in these organelles. As a result, metabolic products of lower molecular weight are formed which can either remain trapped or be released from these compartments. These observations are consistent with our previous results that show that porphyrin−peptide conjugates are found mainly in the lysosomes[21,30,50] and that PEG−porphyrin **1**, *m*/*z* 1066, one of the metabolic products identified in this experiment, is mainly found in the ER.[39]

Experimental Section

Chemistry. Unless otherwise indicated, all commercially available starting materials were used directly without further purification. NMR spectra (see the Supporting Information) were obtained on either a Varian INOVA-500 or a Varian VS-700 instrument. Chemical shifts (δ) are given in ppm relative to TMS. Electronic absorption spectra were measured on a Perkin-Elmer Lambda 35 UV–vis spectrophotometer. Mass spectra were obtained on a Bruker ProFLEX III MALDI-TOF mass spectrometer with a MALDI ionization source using CCA as the matrix. HPLC separation and analysis were performed on a Dionex system including a P680 pump and UVD340U detector. Semipreparative HPLC was carried out using a Luna C_{18} 100 Å, 5 μm, 10 × 250 mm (Phenomenex, Torrance, CA) column and a stepwise gradient; analytical HPLC was carried out using a Delta Pak C_{18} 300 Å, 5 μm, 3.9 × 150 mm (Waters, Milford, MA) column and a stepwise gradient.

Peptide Synthesis. The peptide sequences were prepared on an automated peptide synthesizer (Applied Biosystems Pioneer, Peptide Synthesis System, Foster City, CA) on a 0.2 mmol scale, using the Fmoc strategy of solid-phase peptide synthesis. A 4-fold excess of the Fmoc-protected amino acids were coupled to the PAL-PEG-PS resin using PyBOP as the activating agent. The peptide sequences prepared using this methodology were as follows: RQIKIWFQNRRMKWKKAPPKKKRKVG, KRPAATKKAGQAKKKLEDPRKKRRQRRRPPQG, MGLGLHLLVLAAALQGAWSQAPPKKKRKVG, and APPKKKRKVEDPRKKRRQRRRPPQG. After the final coupling and the successive removal of the Fmoc group, the resin was washed with DMF and isopropyl alcohol and then dried under vacuum. The dried resins containing the protected amino acid sequences were used in the coupling reaction to the porphyrin derivatives.

1. Syntheses of Porphyrin−Peptide Conjugates (General Procedure). Peptidyl resin (0.025 mmol) was introduced into a glass synthesizer, swelled in DMF for 1 h, and then washed with DMF (2 × 5 mL). To the peptidyl resin was added 500 μL of a solution containing 0.05 mmol of porphyrin **1**, 0.150 mmol of DIEA, 0.05 mmol of HOBt, and 0.05 mmol of TBTU. The reaction mixture was shaken overnight at room temperature and then filtered to give a dark purple resin. The resin was washed to remove unreacted porphyrin, first with DMF until the filtrate was colorless and then with dichloromethane and methanol, before being dried under vacuum. Cleavage and deprotection was carried out by treatment of the dried resin with 3 mL of a mixture of TFA/phenol/TIS/H_2O, 88/5/2/5, at room temperature for 4 h. The resin was filtered and washed with TFA (3 × 2 mL), and the filtrates were combined and evaporated under vacuum to give a green residue. Addition of cold Et_2O yielded a green precipitate, which was washed repeatedly with Et_2O and dried under vacuum. The purification of the porphyrin conjugates was achieved by reversed-phase HPLC on a Luna C_{18} semipreparative column (10 × 250 mm, 5 μm) (Phenomenex, Torrance, CA) using a solvent system of water/acetonitrile both containing 0.1% TFA, with a stepwise gradient from 20 to 95%. The fraction containing the conjugate was collected and lyophilized to yield pure conjugate. The purity of the peptides was >95% as obtained by HPLC on an analytical Delta Pak C_{18} (3.9 × 150 mm, 5 μm) column.

Pegylated Porphyrin 1. This porphyrin was synthesized as we have previously reported.[21]

Porphyrin−Peptide Conjugate 2: yield 72%; HPLC t_R = 10.21 min; UV–vis (MeOH) λ_{max} (ε/M^{-1} cm^{-1}) 415 (277000), 512 (15200), 547 (9100), 588 (6800), 645 (7700); LRMS (MALDI) *m*/*z* 4192.312 (M + H^+), calcd for $C_{196}H_{302}N_{62}O_{42}$ 4196.340.

Porphyrin−Peptide Conjugate 3: yield 18%; HPLC t_R = 21.76 min; UV–vis (MeOH) λ_{max} (ε/M^{-1} cm^{-1}) 414 (301000), 513 (16000), 547 (10000), 588 (7600), 645 (6600); LRMS (MALDI) *m*/*z* 4189.436 (M + H^+), calcd for $C_{206}H_{305}N_{49}O_{43}S$ 4188.050.

Porphyrin−Peptide Conjugate 4: yield 30%; HPLC t_R = 17.03 min; UV–vis (MeOH) λ_{max} (ε/M^{-1} cm^{-1}) 414 (313900), 512 (16200), 547 (10000), 589 (7600), 645 (6400); LRMS (MALDI) *m*/*z* 4437.457 (M + H^+), calcd for $C_{218}H_{323}N_{59}O_{40}S$ 4439.470.

Porphyrin−Peptide Conjugate 5: yield 52%; HPLC t_R = 8.85 min; UV–vis (MeOH) λ_{max} (ε/M^{-1} cm^{-1}) 414 (298400), 512 (15200), 547 (9300), 589 (7000), 645 (5800); LRMS (MALDI) *m*/*z* 4812.311 (M + H^+), calcd for $C_{222}H_{353}N_{71}O_{50}$ 4813.726.

2. CD Studies. The CD measurements were carried out on a AVIV 620S circular dicroism spectrometer using 1 mm path length quartz cells. Porphyrin−peptide conjugate solutions (20 μM) were prepared in water/TFE 9/1, pH 7.00, 50 mM NaH_2PO_4 pH 5.00, and 100 mM SDS/H_2O, pH 3.70. All spectra correspond to an average of three separate experiments and were corrected by the baseline obtained for porphyrin−peptide conjugate-free solutions.

3. Cell Culture. All tissue culture media and reagents were obtained from Invitrogen. Human HEp2 cells were obtained from ATCC and maintained in a 50:50 mixture of DMEM/Advanced MEM containing 5% FBS. The cells were subcultured biweekly to maintain subconfluent stocks.

3.1. Time-Dependent Cellular Uptake. HEp2 cells were plated at 10000 per well in a Costar 96 well plate and allowed to grow for 36 h. Conjugate stocks were prepared in water at a concentration of 10 mM and then diluted into medium to final working concentrations. The cells were exposed to 10 μM of each conjugate for 0, 1, 2, 4, 8, and 24 h. At the end of the incubation time, the loading medium was removed and the cells were washed with 200 μL of PBS. The cells were solubilized upon addition of 100 μL of 0.25% Triton X-100 (Calbiochem, San Diego, CA) in PBS. To determine the conjugate concentration, fluorescence emission was read at 440/650 nm (excitation/emission) using a BMG FLUOstar plate reader. The cell numbers were quantified using the CyQuant reagent (Molecular Probes, Carlsbad, CA).

3.2. Dark Cytotoxicity. The HEp2 cells were plated as described above and allowed 36–48 h to attach. The cells were exposed to increasing concentrations of conjugate up to 100 μM and incubated overnight. The loading medium was then removed and the cells fed with medium containing Cell Titer Blue (Promega, Madison, WI) as per the manufacturer's instructions. Cell viability was then measured by reading the fluorescence at 520/584nm using a BMG FLUOstar plate reader. The signal was normalized to 100% viable (untreated) cells and 0% viable (treated with 0.2% saponin from Sigma) cells.

3.3. Phototoxicity. The HEp2 cells were prepared as described above for the dark cytotoxicity assay and treated with conjugate concentrations of 0, 0.625, 1.25, 2.5, 5, and 10 μM. After compound loading, the medium was removed and replaced with medium containing 50 mM HEPES pH 7.4. The cells were then placed on ice and exposed to light from a 100 W halogen lamp filtered through a 610 nm long pass filter (Chroma) for 20 min. An inverted plate lid filled with water to a depth of 5 mm acted as an IR filter. The total light dose was approximately 1 J/cm^2. The cells were returned to the incubator overnight and assayed for viability as described above for the dark cytotoxicity experiment.

3.4. Intracellular Localization. The HEp2 cells were plated on LabTek 2 chamber coverslips and incubated overnight, before being exposed to 10 μM of conjugate for 18 h. For the colocalization experiments the cells were incubated for 18 h concurrently with conjugate and one of the following organelle tracers, for 30 min: MitoTracker Green (mitochondria) 250 nM, LysoSensor Green (lysosomes), 50 nM, $DiOC_6$ (ER) 5 μg/mL, BODIPY FL C_5-ceramide at 50 nM (Golgi network). The slides were washed three times with growth medium and new medium containing 50 mM HEPES pH 7.4 was added. Fluorescent microscopy was performed using a Zeiss Axiovert 200 M inverted fluorescent microscope fitted with standard FITC and Texas Red filter sets (Chroma). The images were aquired with a Zeiss Axiocam MRM CCD camera fitted to the microscope.

4. Hydrolysis Studies. Cathepsin B EC 3.4.22.1, cathepsin D, EC 3.4.23.5, prolidase EC 232.791.5, and plasmin EC 3.4.21.7 were obtained from Sigma-Aldrich as lyophilized powders.

4.2. Nonenzymatic Hydrolysis. Stability at pH 7.4: 100 μM solution of each conjugate in 50 mM PBS pH 7.4 was incubated for 24 h at 37 °C. Stability at pH 5.0: 100 μM solution of each conjugate in 50 mM acetate buffer pH 5.0 was incubated for 24 h at 37 °C. The hydrolysis products were identified by MALDI-TOF mass spectroscopy using CCA as the matrix.

4.2. Enzymatic Hydrolysis. Cathepsin B EC 3.4.22.1 from bovine spleen (10 units) was dissolved in 1 mL of 50 mM NaOAc, 1 mM EDTA buffer pH 5.4. To 100 μL of cathepsin B solution were added 5 μL of 1 M DTT and 10 μL of 1 mM conjugate solution. The mixture was incubated at 37 °C for 24 h. Enzymatic activity was stopped by the addition of 50 μL of 50 mM phosphate buffer pH 8.5. Cathepsin D, EC 3.4.23.5 from bovine spleen (5 units) was dissolved in 500 μL of distilled water. To 50 μL of cathepsin D solution were added 15 μL of water, 10 μL of 1 N formate buffer pH 3.8, and 10 μL of 1 mM conjugate solution. The mixture was incubated at 37 °C for 24 h. Enzymatic activity was stopped by the addition of 100 μL of 50 mM phosphate buffer pH 8.5. Prolidase EC 232.791.5 was prepared to a working solution of 1 unit/100 μL in 50 mM Tris−HCl buffer pH 7.4 containing 10 mM $MnCl_2$. To 50 μL of the prolidase working solution was added 5 μL of 1 mM conjugate solution. The mixture was incubated at 37 °C for 24 h. Enzymatic activity was stopped by the addition of 20 μL of TFA. Plasmin EC 3.4.21.7 was prepared to a working solution of 1 unit/100 μL in 100 mM Tris−HCl buffer pH 7.4. To a 50 μL of the plasmin working solution was added 5 μL of 1 mM conjugate solution. The mixture was incubated at 37 °C for 24 h. Enzymatic activity was stopped by the addition of 20 μL of TFA. The hydrolysis products were identified by MALDI-TOF mass spectroscopy using CCA as the matrix.

4.3. Time-Dependent Conjugate Hydrolysis in Cell Culture. HEp2 cells were plated at 60000 per well in a B & D 24 well plate and allowed to grow for 36 h. Conjugate **5** stock solution was prepared in water at a concentration of 10 mM and then diluted into medium to final working concentrations. The cells were exposed to 10 μM of conjugate **5** for 1, 2, 4, 8, and 24 h. At the end of the incubation period, the loading medium was removed and the cells were washed with PBS (5 × 1 mL). MeOH/H_2O 1:1 (500 μL) containing 0.1% TFA was added to each well. From each well, the cells were scraped with the aid of a cell scraper and the resulting suspension transferred to a centrifuge tube. The suspension was centrifuged, and the cell pellet was washed with MeOH/H_2O 1:1 containing 0.1% TFA (5 × 300 μL) until the supernatant was colorless. Washings for each time were pooled and concentrated by lyophilization. The green solid residue was redissolved in 50 μL of acetonitrile/H_2O 1:1 containing 0.1% TFA and analyzed by HPLC and MALDI-TOF mass spectroscopy.

Conclusions

We have synthesized a series of four new porphyrin−peptide conjugates bearing a linear bifunctional peptide containing both CPP and NLS sequences. Our results show that the cellular uptake and cytotoxicity of these conjugates in human carcinoma HEp2 cells depends on the nature and sequence of the amino acid residues and the hydrophobic character of the conjugate; the least hydrophobic conjugates **2** and **5** bearing a NLS (SV40 or nucleoplasmin, respectively) and the CPP HIV-1 Tat 48–60 accumulated the most within HEp2 cells and were the most phototoxic. All conjugates are highly stable in the absence of proteolytic enzymes, but their peptide chains are cleaved to some extent in multiple places (no specific pattern was observed) by enzymes within tumor cells, including cathepsin B, cathepsin D, prolidase, and plasmin. It is concluded that porphyrin−peptide conjugates bearing a CPP sequence with multiple arginine residues (e.g., the HIV-1 Tat 48–60) are efficiently taken up by HEp2 cells, possibly via an endocytotic mechanism, and remain trapped in the cell endosomes and lysosomes, where some degradation of the peptide chain occurs. As a consequence, the preferential sites of subcellular localization of the porphyrin−peptide conjugates are the endosomes, lysosomes, and the ER, the latter probably targeted by porphyrin−PEG-containing fragment(s).

Acknowledgment. We thank Martha Juban for peptide sequence syntheses and Dr. Thomas K. Weldeghiorghis for

NMR data acquisition. This work was partially supported by the National Science Foundation, Grant No. CHE-304833.

Supporting Information Available: ^{1}H NMR, COSY, DQF-COSY, and TOCSY spectra for all porphyrins, HPLC traces, and fluorescence microscopy images for all porphyrins, Tables with possible hydrolysis products from enzymatic hydrolysis, MALDI-TOF, and UV–vis spectra of hydrolysis products from porphyrin-peptide conjugate **5**. This material is available free of charge via the Internet at http://pubs.acs.org.

References

(1) Pandey, R. K., Zheng, G. Porphyrins as photosensitizers in photodynamic therapy. In *The Porphyrin Handbook*; Kadish, K. M., Smith, K. M., Guilard, R., Eds.; Academic Press: Boston, MA, 2000; Vol. 6, pp 157–230.

(2) Brown, S. B.; Brown, E. A.; Walker, I. The present and future role of photodynamic therapy in cancer treatment. *Lancet Oncol.* **2004**, *5*, 497–58.

(3) Barth, R. F.; Coderre, J. A.; Vicente, M. G. H.; Blue, T. E. Boron neutron capture therapy of cancer: current status and future prospects. *Clin. Cancer Res.* **2005**, *11*, 3987–4002.

(4) Kessel, D. Correlation between subcellular localization and photodynamic efficacy. *J. Porphyrins Phthalocyanines* **2004**, *8*, 1009–1014.

(5) Rosenkranz, A. A.; Jans, D. A.; Sobolev, A. S. Targeted intracellular delivery of photosensitizers to enhance photodynamic efficiency. *Immunol. Cell Biol.* **2002**, *78*, 452–464.

(6) Osterloh, J.; Vicente, M. G. H. Mechanisms of Porphyrinoid Localization in Tumors. *J. Porphyrins Phthalocyanines* **2002**, *6*, 305–324.

(7) Soini, A. E.; Yashunsky, D. V.; Meltola, N. J.; Ponomarev, G. V. Influence of linker unit on performance of palladium(II) coproporphyrin labelling reagent and its bioconjugates. *Luminescence* **2003**, *18*, 182–92.

(8) Li, H.; Fedorova, O. S.; Trumble, W. R.; Fletcher, T. R.; Czuchajowski, L. Site-specific photomodification of DNA by porphyrin-oligonucleotide conjugates synthesized via a solid phase H-phosphonate approach. *Bioconjugate Chem.* **1997**, *8*, 49–56.

(9) (a) Mestre, B.; Jakobs, A.; Pratviel, G.; Meunier, B. Structure/nuclease activity relationships of DNA cleavers based on cationic metalloporphyrin-oligonucleotide conjugates. *Biochemistry* **1996**, *35*, 9140–9149. (b) Mestre, B.; Pitie, M.; Loup, C.; Claparols, C.; Pratviel, G.; Meunier, B. Influence of the nature of the porphyrin ligand on the nuclease activity of metalloporphyrin-oligonucleotide conjugates designed with cationic, hydrophobic or anionic metalloporphyrins. *Nucleic Acids Res.* **1997**, *25*, 1022–1027.

(10) (a) Del Governatore, M.; Hamblin, M. R.; Piccinini, E. E.; Ugolini, G.; Hasan, T. Targeted photodestruction of human colon cancer cells using charged 17.1A chlorin e6 immunoconjugates. *Br. J. Cancer* **2000**, *82*, 56–64. (b) Hamblin, M. R.; Del Governatore, M.; Rizvi, I.; Hasan, T. Biodistribution of charged 17.1A photoimmunoconjugates in a murine model of hepatic metastasis of colorectal cancer. *Br. J. Cancer* **2000**, *83*, 1544–1551.

(11) Hudson, R.; Carcenac, M.; Smith, K.; Madden, L.; Clarke, O. J.; Pelegrin, A.; Greenman, J.; Boyle, R. W. The development and characterization of porphyrin isothiocyanate-monoclonal antibody conjugates for photoimmunotherapy. *Br. J. Cancer* **2005**, *92*, 1442–1449.

(12) (a) Gijsens, A.; De Witte, P. Photocytotoxic action of EGF-PVA-Sn(IV)chlorin e6 and EGF-dextran-Sn(IV)chlorin e6 internalizable conjugates on A431 cells. *Int. J. Oncol.* **1998**, *13*, 1171–1177. (b) Gijsens, A.; Missiaen, L.; Merlevede, W.; de Witte, P. Epidermal growth factor-mediated targeting of chlorin e6 selectively potentiates its photodynamic activity. *Cancer Res.* **2000**, *60*, 2197–2202.

(13) Chen, X.; Hui, L.; Foster, D. A.; Drain, C. M. Efficient synthesis and photodynamic activity of porphyrin-saccharide conjugates: targeting and incapacitating cancer cells. *Biochemistry* **2004**, *43*, 10918–10929.

(14) Li, G.; Pandey, S. K.; Graham, A.; Dobhal, M. P.; Mehta, R.; Chen, Y.; Gryshuk, A.; Rittenhouse-Olson, K.; Oseroff, A.; Pandey, R. K. Functionalization of OEP-based benzochlorins to develop carbohydrate-conjugated photosensitizers. Attempt to target beta-galactoside-recognized proteins. *J. Org. Chem.* **2004**, *69*, 158–172.

(15) (a) Lundberg, P.; Langel, U. A brief introduction to cell-penetrating peptides. *J. Mol. Recognit.* **2003**, *16*, 227–233. (b) Richard, J. P.; Melikov, K.; Vives, E.; Ramos, C.; Verbeure, B.; Gait, M. J.; Chernomordik, L. V.; Lebleu, B. Cell-penetrating Peptides: A Reevaluation of the mechanism of cellular uptake. *J. Biol. Chem.* **2003**, *278*, 585–590. (c) Futaki, S.; Goto, S.; Suzuki, T.; Nakase, I.; Sugiura, Y. Structural variety of membrane permeable peptides. *Curr. Protein Peptide Sci.* **2003**, *4*, 87–96. (d) Schwartz, J. J.; Zhang, S. Peptide-mediated cellular delivery. *Curr. Opin. Mol. Ther.* **2000**, *2*, 162–167.

(16) Derossi, D.; Joliot, A.; Chassaing, G.; Prochiantz, A. The third helix of the Antennapedia homeodomain translocates through biological membranes. *J. Biol. Chem.* **1994**, *269*, 10444–10450.

(17) Vives, E. Cellular uptake of the Tat peptide: an endocytosis mechanism following ionic interactions. *J. Mol. Recognit.* **2003**, *16*, 265–271.

(18) (a) Normand, N.; van Leeuwen, H.; O'Hare, P. Particle formation by the HSV protein VP22 enabling protein and nucleic acid delivery. *J. Biol. Chem.* **2001**, *276*, 15042–15050. (b) Brewis, N. D.; Phelan, A.; Normand, N.; Choolun, E.; O'Hare, P. Particle assembly incorporating a VP22-BH3 fusion protein, facilitating intracellular delivery, regulated release, and apoptosis 1. *Mol. Ther.* **2003**, *7*, 262–270.

(19) (a) Mitchell, D. J.; Kim, D. T.; Steinman, L.; Fathman, C. G.; Rothbard, J. B. Polyarginine enters cells more efficiently than other polycationic homopolymers. *J. Peptide Res.* **2000**, *56*, 318–325. (b) Rothbard, J. B.; Jessop, T. C.; Lewis, R. S.; Murray, B. A.; Wender, P. A. Role of membrane potential and hydrogen bonding in the mechanism of translocation of guanidinium-rich peptides into cells. *J. Am. Chem. Soc.* **2004**, *126*, 9506–9507. (c) Futaki, S.; Ohashi, W.; Suzuki, T.; Niwa, M.; Tanaka, S.; Ueda, K.; Harashima, H.; Sugiura, Y. Stearylated arginine-rich peptides: A new class of transfection systems. *Bioconjugate Chem.* **2001**, *12*, 1005–1011.

(20) Boulikas, T. Nuclear localization signals. *Crit. Rev. Eukariotic Gene Expression* **1993**, *3*, 193–227.

(21) Sibrian-Vazquez, M.; Jensen, T. J.; Hammer, R. P.; Vicente, M. G. H. Peptide-mediated cell transport of water soluble porphyrin conjugates. *J. Med. Chem.* **2006**, *49*, 1364–1372.

(22) Prado, A.; Ramos, I.; Frehlick, L. J.; Muga, A.; Ausio, J. Nucleoplasmin: a nuclear chaperone. *Biochem. Cell Biol.* **2004**, *82*, 437–445.

(23) (a) Akhlynina, T. V.; Jans, D. A.; Rosenkranz, A. A.; Statsyuk, N. V.; Balashova, I. Y.; Toth, G.; Pavo, I.; Rubin, A. B.; Sobolev, A. S. Nuclear targeting of chlorin e6 enhances its photosensitizing activity. *J. Biol. Chem.* **1997**, *272*, 20328–20331. (b) Akhlynina, T. V.; Jans, D. A.; Statsyuk, N. V.; Balashova, I. Y.; Toth, G.; Pavo, I.; Rosenkranz, A. A.; Naroditsky, B. S.; Sobolev, A. S. Adenoviruses synergize with nuclear localization signals to enhance nuclear delivery and photodynamic action of internalizable conjugates containing chlorin e6. *Int. J. Cancer* **1999**, *81*, 734–740.

(24) Chaloin, L.; Bigey, P.; Loup, C.; Marin, M.; Galeotti, N.; Piechaczyk, M.; Heitz, F.; Meunier, B. Improvement of porphyrin cellular delivery and activity by conjugation to a carrier peptide. *Bioconjugate Chem.* **2001**, *12*, 691–700.

(25) Bisland, S. K.; Singh, D.; Gariepy, J. Potentiation of chlorin e6 photodynamic activity in vitro with peptide-based intracellular vehicles. *Bioconjugate Chem.* **1999**, *10*, 982–992.

(26) Deshayes, S.; Morris, M. C.; Divita, G.; Heitz, F. Cell-penetrating peptides: tools for intracellular delivery of therapeutics. *Cell. Mol. Life. Sci.* **2005**, 1839–1849.

(27) Futaki, S.; Goto, S.; Suzuki, T.; Nakase, I.; Sugiura, Y. Structural variety of membrane permeable peptides. *Curr. Protein Peptide Sci.* **2003**, *4*, 87–96.

(28) Dietz, G. P.; Bahr, M. Delivery of bioactive molecules into the cell: the Trojan horse approach. *Mol. Cell. Neurosci.* **2004**, *27*, 85–131.

(29) Vives, E. Present and future of cell-penetrating peptide mediated delivery systems: "Is the Trojan horse to wild to go only to Troy?". *J. Controlled Release* **2005**, *109*, 77–85.

(30) Sibrian-Vazquez, M.; Jensen, T. J.; Fronczek, F. R.; Hammer, R. P.; Vicente, M. G. H. Synthesis and characterization of positively charged porphyrin-peptide conjugates. *Bioconjugate Chem.* **2005**, *16*, 852–863.

(31) Greenwald, R. B.; Choe, Y. H.; McGuire, J.; Conover, C. D. Effective drug delivery by pegylated drug conjugates. *Adv. Drug Deliv. Rev.* **2003**, *55*, 217–250.

(32) (a) Hamblin, M. R.; Miller, J. L.; Rizvi, I.; Ortel, B.; Maytin, E. V.; Hasan, T. Pegylation of a chlorin(e6) polymer conjugate increases tumor targeting of photosensitizer. *Cancer Res.* **2001**, *61*, 7155–7162. (b) Kim, Y. S.; Song, R.; Hyun Kim, D.; Jun, M. J.; Sohn, Y. S. Synthesis, biodistribution and antitumor activity of hematoporphyrin-platinum(II) conjugates. *Bioorg. Med. Chem.* **2003**, *11*, 1753–1760.

(33) Greenfield, N.; Fasman, G. D. Computed circular dichroism spectra for the evaluation of protein conformation. *Biochemistry* **1969**, *8*, 4108–4116.

(34) Conti, E.; Uy, M.; Leighton, L.; Blobel, G.; Kuriyan, J. Crystallographic analysis of the recognition of a nuclear localization signal by the nuclear import facto kariopherin α. *Cell* **1988**, *94*, 193–204.

(35) (a) Fontes, M. R. M.; Teh, T.; Kobe, B. Structural basis of recognition of monopartite and bipartite nuclear localization sequences by mammalian importin-alpha. *J. Mol. Biol.* **2000**, *297*, 1183–1194. (b) Fontes, M. R. M.; Teh, T.; Jans, D.; Brinkworth, R. I.; Kobe, B. Structural basis for the specificity of bipartite nuclear localization sequence binding by importin-alpha. *J. Biol. Chem.* **2003**, *278*, 27981–27987.

(36) Loret, E. P.; Vives, E.; Pui Shing Ho, P. S.; Rochat, H.; van Rietschoten, J.; Johnson Jr., W. C. Activating region of HIV-1 Tat protein: vacuum UV circular dichroism and energy minimization. *Biochemistry* **1991**, *30*, 6013–6023.

(37) (a) Lindber, M.; Graslund, A. The position of the cell penetrating peptide penetratin in SDS micelles determined by NMR. *FEBS Lett.* **2001**, *497*, 39–44. (b) Persson, D.; Thoren, P. E. G.; Norden, B. Penetratin-induced aggregation and subsequent dissociation of negatively charged phospholipids vesicles. *FEBS Lett.* **2001**, *505*, 307–312. (c) Berlose, J-P.; Convert, O.; Derossi, D.; Brunissen, A.; Chassaing, G. Conformational and associative behaviours of the third helix of antennapedia homeodomain in membrane-mimetic environments. *Eur. J. Biochem.* **1996**, *242*, 372–386. (d) Balayssac, S.; Burlina, F.; Convert, O.; Bolbach, G.; Chassaing, G.; Lequin, O. Comparison of penetratin and other homeodomain-divided cell-penetrating peptides: Interation in membrane-mimicking environment and cellular uptake efficiency. *Biochemistry* **2006**, *45*, 1408–1420.

(38) (a) Rizzo, J.; Blanco, F. J.; Kobe, B.; Bruch, M. D.; Gierasch, M. Conformational behavior of Escherichia coli OmpA signal peptides in membrane mimicking environments. *Biochemistry* **1993**, *32*, 4881–4894. (b) Chaolin, L.; Vidal, P.; Heitz, A.; van Mau, N.; Mery, J.; Divita, G.; Heitz, F. Conformations of primary amphiphatic carrier peptides in membrane mimicking environments. *Biochemistry* **1997**, *36*, 11179–11187.

(39) Sibrian-Vazquez, M.; Jensen, T. J.; Vicente, M. G. H. Synthesis and cellular studies of PEG-functionalized meso-tetraphenylporphyrins. *J. Photochem. Photobiol. B: Biol.* **2007**, *86*, 9–21.

(40) Linder, S.; Shoshan, M. C. Lysosomes and endoplasmic reticulum: targets for improved, selective anticancer therapy. *Drug Resist. Updates* **2005**, *8*, 199–204.

(41) Tardy, C.; Codogno, P.; Autefage, H.; Levade, T.; Andrieu-Abadie, N. Lysosomes and lysosomal proteins in cancer cell death (new players of an old struggle). *Biochim. Biophys. Acta* **2006**, *1765*, 101–125.

(42) (a) Ajit, J. M.; D'Souza, M. T. Release from polymeric prodrugs: Linkages and their degradation. *J. Pharm. Sci.* **2004**, *93*, 1962–1979. (b) Ekins, S.; Ring, B. J.; Grace, J.; McRobie-Belle, D. J.; Wrighton, S. A. Present and future in vitro approaches for drug metabolism. *J. Pharmacol. Toxicol. Methods* **2000**, *44*, 313–324.

(43) Smith, R. M.; Hansen, D. E. The pH−rate profile for the hydrolysis of a peptide bond. *J. Am. Chem. Soc.* **1998**, *120*, 8910–8913.

(44) Radzicka, A.; Wolfenden, R. Rates of uncatalyzed peptide bond hydrolysis in neutral solution and the transition state affinities of proteases. *J. Am. Chem. Soc.* **1996**, *118*, 6105–6109.

(45) Thomssen, C.; Schmitt, M.; Goretzki, L.; Oppelt, P.; Pache, L.; Dettmar, P.; Janicke, F.; Graeff, H. Prognostic value of the cysteine proteases cathepsins B and cathepsin L in human breast cancer. *Clin. Cancer Res.* **1995**, *1*, 741–746.

(46) Bielawska, A.; Bielawski, K.; Chrzanowski, K.; Wolczynski, S. Prolinase-activated pro-drug for cancer chemotherapy. Cytotoxic activity of proline analogue of chlorambucil in breast cancer MCF-7 cells. *Farmaco* **2000**, *55*, 736–741.

(47) Toki, B. E.; Cerveny, C. G.; Wahl, A. F.; Senter, P. D. Protease-mediated fragmentation of p-amidobenzyl ethers: a new strategy for the activation of anticancer prodrugs. *J. Org. Chem.* **2002**, *67*, 1866–1872.

(48) (a) de Groot, F. M. H.; van Berkom, L. W. A.; Scheeren, H. W. Synthesis and biological evaluation of 2′-carbamate-linked and 2′-carbonate-linked prodrugs of paclitaxel: selective activation by the tumor-associated protease plasmin. *J. Med. Chem.* **2000**, *43*, 3093–3102. (b) Andreasen, P. A.; Egelund, R.; Peterson, H. H. The plasminogen activation system in tumor growth, invasion, and metastasis. *Cell. Mol. Life Sci.* **2000**, *57*, 25–40.

(49) (a) Want, E. J.; Cravatt, B. F.; Siuzdak, G. The expanding role of mass spectrometry in metabolite profiling and characterization. *Chem. Biol. Chem.* **2005**, *6*, 1941–1951. (b) May, L. A.; Tourkina, E.; HoVmanb, S. R.; Dix, T. A. Detection and quantitation of curcumin in mouse lung cell cultures by matrix-assisted laser desorption ionization time of flight mass spectrometry. *Anal. Biochem.* **2005**, *33*, 762–769.

(50) Sibrian-Vazquez, M.; Nesterova, I. V.; Jensen, T. J.; Vicente, M. G. H. Mitochondria-Targeting by Guanidine-and Biguanidine-Porphyrin Photosensitizers. *Bioconjugate Chem.* **2008**, *19*, 705–713.

JM701050J